DESIGN AND FABRICATION OF AN ACTIVE MEMBRANE DESALINATION MODULE

A Senior Honors Thesis

Presented in Partial Fulfillment of the Requirements for Graduation with Distinction in the Department of Mechanical and Aerospace Engineering in the Undergraduate Colleges at The Ohio State University

By

Cameron Bodenschatz

The Ohio State University

18 May 2012

Examination Committee: Approval:

Dr. Shaurya Prakash, Advisor _____

Dr. Robert Siston _____

ABSTRACT

Water shortage is a growing problem that continues to affect people worldwide. According to the Intergovernmental Panel on Climate Change, over 1.2 billion people live in areas that face a physical scarcity of water and another 1.6 billion people live in areas lacking the infrastructure to distribute water. Of the current major desalination methods, membrane separations are favorable to distillation methods due to relatively lower energy requirements. However, they are also subject to irreversible membrane fouling and reduction in flux due to concentration polarization, which leads to less efficient separation. The purpose of this study is to implement a new approach for mitigating concentration polarization, often considered the precursor to membrane fouling, in order to maintain higher efficiency of reverse osmosis salt removal over extended periods of time. A disc tube (DT) reverse osmosis (RO) module based on a commercial Pall-DT system was modified for in-lab testing of this method, which consists of applying an alternating potential to a metalized polymer RO membrane. Our hypothesis was that the AC potential causes a local convective loop formation due to small perturbations to the ion concentration polarization layer as the AC frequency is matched to the typical diffusion time of ions within a few microns of the membrane surfaces. These convective loops generate local mixing regions thereby reducing the effective thickness of the polarization region and improving membrane flux. Fabrication of the RO module included several troubleshooting steps, and the final module is capable of achieving salt rejections of approximately 90%. Testing of the RO module with an applied electrical bias yielded a permeate water flux increase of roughly 14% at a power consumption of 2.7 W.

DEDICATION

This work is dedicated to my family and friends, for pushing me and helping me to be the best that I can be.

ACKNOWLEDGEMENTS

I would like to thank Dr. Shaurya Prakash, Ms. Karen Bellman, and Dr. Robert Siston for providing endless assistance, guidance, and encouragement. I would also like to thank the researchers at the Microsystems and Nanosystems (MSNS) Lab and the class members of ME 783H for all of their support along the course of this project. Financial support or in-kind services were provided by the following institutions and companies: The Ohio State University, The Ohio State University College of Engineering, and the MSNS Lab.

TABLE OF CONTENTS

LIST OF FIGURES

LIST OF TABLES

LIST OF EQUATIONS

1. INTRODUCTION

1.1 PURPOSE

Concentration polarization is due to the adsorption of solute particles in a solution onto the surface and into the pores of a membrane. The adsorption process can be governed by many parameters in membrane filtration including membrane selectivity properties, surface charge density, and permeability of the membrane, among others. The solute particles physically block solvent molecules from passing through the pores of the membrane, decreasing the membranes permeability and measured flux. This requires a higher driving force to push solvent molecules across the membrane, resulting in higher energy requirements and costs. The purpose of this project specifically is to design and fabricate a laboratory scale reverse osmosis unit to test the effects of an electrical concentration polarization mitigation technique on permeate water flux.

1.2 WORLD WATER RESOURCES

Freshwater is an extremely valuable and necessary resource all around the world and a region's ability to distribute purified freshwater is a major indicator of its ability to thrive. Given that approximately 70% of the planet is covered in water and that water returns to a useable form through natural processes such evapotranspiration, it would seem that there is plenty of water to supply all of the potential needs [1]. However, of the approximately 1.4×10^{21} L of total water on Earth, only about 2.5% is freshwater, as seen in Figure 1 [2]. The other 97.5% is saltwater that exists in oceans, bays, seas, and saline aquifers and is not able to be used in the naturally occurring form. Of the total available freshwater on Earth, approximately 70% is present as ice and snow cover in mountainous regions, and is therefore essentially inaccessible, as seen in Figure 2 [2]. A rough estimate

is that only 0.7% of the total water on Earth, approximately 9.8×10^{18} L, is readily available for use as freshwater [3]. It is estimated that 3.8×10^{15} L of water is that withdrawn annually by humans for a variety of modern society endeavors such as agriculture, energy generation, and potable human use. However, withdrawals such as evapotranspiration and animal and plant uses are not taken into consideration in this number. Also not shown by this number are variations based on region, climate, and time of the year.

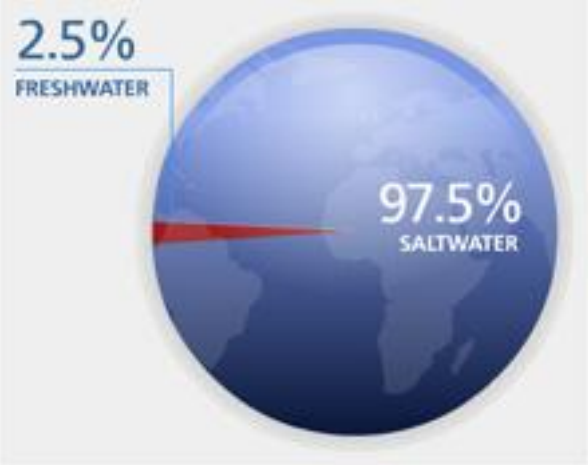

Figure 1: Breakdown of total world water resources [2].

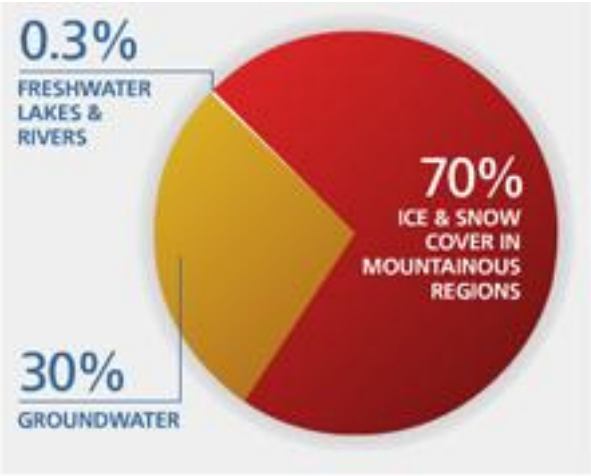

Figure 2: Breakdown of world freshwater resources [2].

A 2007 study by the Intergovernmental Panel on Climate Change shows that 1.2 billion people live in areas of physical scarcity of freshwater. The study also shows that an additional 1.6 billion people live in areas lacking the appropriate infrastructure to distribute cleaned freshwater [4]. This means that approximately 40% of the world's population live in areas that do not necessarily have freshwater readily available for use. The effects of this lack of freshwater can be seen in World Health Organization (WHO) reports, which show that approximately 2.4 million people die every year from contaminated water, including a child under the age of 5 every 20 seconds. Many others suffer from waterborne diseases including malaria, cholera, and diarrhea [2]. Therefore it is essential that means of producing clean freshwater for the areas that are affected by these issues are developed. Given that the population is growing at a rate of roughly 80 million people per year, it is projected that the number of people living in water-stressed regions could grow to 3.5 billion people by 2025 [5]. This problem will be especially evident in developing countries where water withdrawals are predicted to increase by 50% by 2025, compared to 18% for developed countries [1].

Drinking water is not the only end use of freshwater. Freshwater is also allocated to various other sectors, including agriculture and industry. Approximately 70% of freshwater withdrawals are for irrigation purposes and about 22% are allocated for industrial uses, including process water and heating and cooling water, as shown by Figure 3 [2]. In these uses, water often gets contaminated with pesticides and industrial waste, leading to further energy consumption for water reuse. Additionally, only about 8% of freshwater withdrawals are allocated for domestic uses and even then the vast majority of domestic uses are for things other than drinking, including running clothes washers, taking

showers, and flushing the toilet, as seen in Figure 4 [6]. It should be noted that even though this data is from a 2005 report, the numbers were actually taken in 1995 because this is the last time the U.S. government collected data on domestic water consumption.

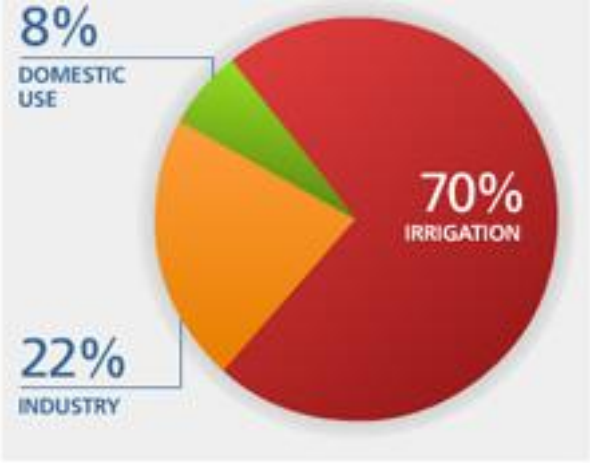

Figure 3: Breakdown of worldwide freshwater use [2].

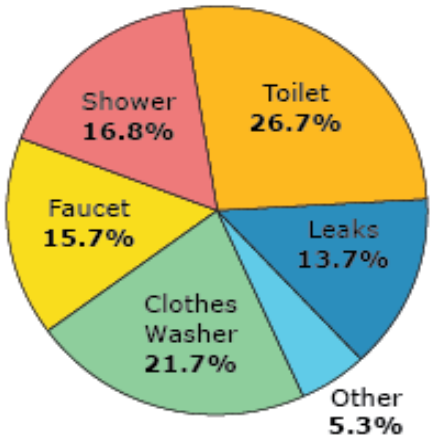

Figure 4: Breakdown of domestic water use by common consumption categories in the US [6].

1.3 TYPES OF WATER

There are three general groups in which source water can be classified based on its level of salinity. Potable water is considered to have less than 0.020 mg/L of total dissolved

solids (TDS). Brackish water has a salinity between that of potable water and that of seawater (but generally ranges between 3,000-10,000 mg/L). This is due to the fact that is found in areas where seawater and freshwater come in contact, such as underground aquifers. Seawater contains roughly 35,000 mg/L of TDS. A summary of the levels of water salinity is shown in Table 1 [7].

Table 1: Salinity and pH of water types [7].

	Potable Water	Brackish Water	Seawater
Salinity (mg/L)	≤0.020	Largely source dependent	35,000
pH	6.5-8.5	Largely source dependent	7.5-8.4

1.4 CURRENT DESALINATION METHODS

There are two major types of desalination methods currently employed to purify water: temperature driven distillation processes and membrane-based processes.

1.4.1 DISTILLATION PROCESSES

Distillation methods of desalination include multistage flash distillation (MSF) and multieffect distillation (MED). Distillation methods work by evaporating the feed water and leaving the salts and other contaminants behind in the concentrated brine stream. The water vapor is the condensed and collected separately from the brine stream as freshwater. Distillation methods of desalination are generally among the most energy intensive because they require large amounts of heat energy to vaporize the water. It can take up to 25 kWh of energy to produce 1 m^3 of freshwater through distillation processes, although through plant improvements including brine recycling and the use of waste heat from other

processes this number continues to drop [5]. The use of waste heat from other processes is a process known as cogeneration, and typically this low-grade waste heat is enough to vaporize water in distillation processes, requiring less direct heating in the form of burning fuel gas to vaporize the inlet water.

Since only water is vaporized and collected in the freshwater stream, salts and other contaminants primarily remain in the liquid brine stream, keeping the amount of fouling relatively low. However, some fouling does still occur in the form of both macro-fouling and micro-fouling. Macro-fouling is the buildup of large particles such as algae cells in the brine reject stream. Micro-fouling is the scaling of calcium and magnesium salts on internal components of the distillation system, typically on the heat exchanging surfaces of the brine heater [3].

An example of a standard MSF plant can be seen in Figure 5 [8]. The inlet seawater comes in cool and is preheated by condensing water vapor from each flash chamber, which is then collected as the freshwater stream. The seawater is then heated the rest of the way to the operating temperature by a heat exchanger which can use steam heated from the waste heat from other processes. As the seawater stream passes through each flash chamber, some of the water vaporizes because the chamber pressure is matched to the vapor pressure of the water stream at its given temperature. Therefore, the brine stream becomes more and more concentrated until it is discharged or recycled

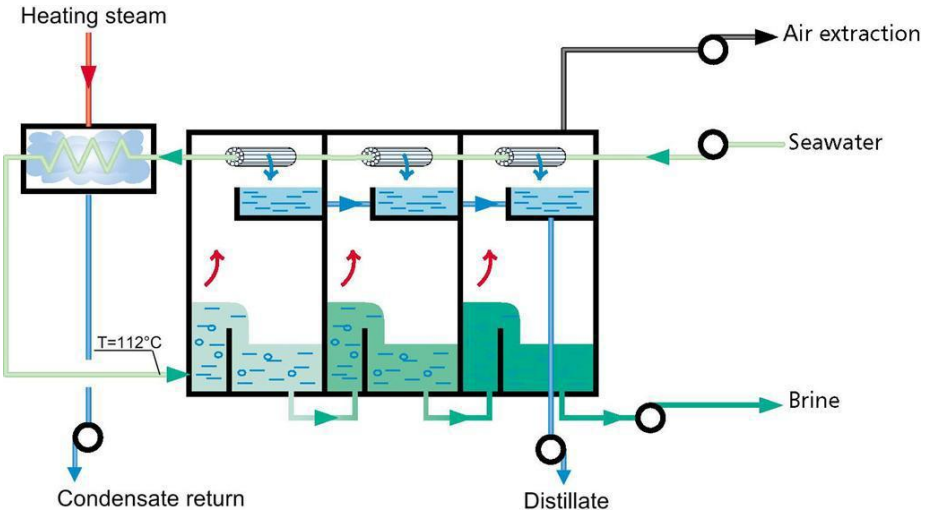

Figure 5: Diagram of a MSF distillation plant [8].

1.4.2 MEMBRANE-BASED PROCESSES

Membrane-based water purification processes typically use semi-permeable polymer membranes as a physical barrier that will allow the flow of water into the purified water stream but block contaminants, including colloids, organic molecules, viruses, and, in the case of desalination, dissolved ions. Membrane-based processes include pressure-driven processes such as ultrafiltration and reverse osmosis, electrically-driven processes such as electrodialysis, and chemical potential-driven processes such as forward osmosis.

Pressure-driven membrane processes are classified based on the size of particle that they allow to pass through the membrane. As seen in Figure 6, membrane separations include microfiltration, ultrafiltration, nanofiltration, and reverse osmosis (RO) in order of decreasing excluded particle size [9]. It can also be seen that as the excluded particle size decreases, a higher operating pressure is required to maintain a high water flux. RO is the only process capable of removing dissolved salt ions from solution, but also requires the highest operating pressure of somewhere between 500 and 900 psi. In fact, RO requires

approximately 1.5-2.5 kWh of energy to produce 1 m^3 of freshwater, approximately 10% of the energy required for distillation processes to produce the same amount of freshwater [5]. This is on the order of magnitude of the theoretical minimum energy required to recover 500 ppm freshwater from 35,000 ppm seawater at a recovery rate of 75%, which is 1.29 kWh/m^3 [3]. This high pressure difference is required to overcome the osmotic pressure difference between the purified water stream and the seawater stream, which for a seawater stream of 35,000 ppm of salt is around 360 psi at a reasonable flux. Typical RO processes can achieve fluxes around 30 L/m^2hr [5].

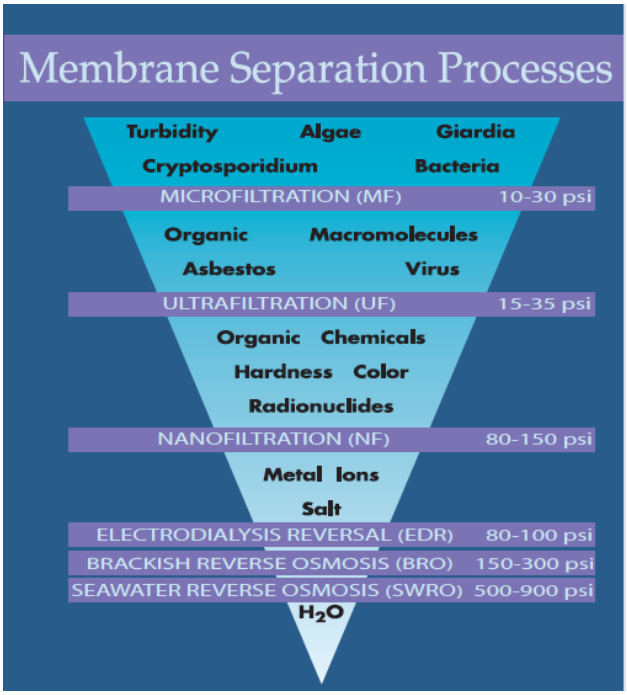

Figure 6: Breakdown of membrane separation processes based on excluded particle size [9].

RO processes are generally modeled using the solution-diffusion model, which assumes that both solute and solvent molecules dissolve into the surface of a nonporous surface layer and then diffuse through the membrane [10]. Therefore it is ideal to have a

membrane in which the solvent has a high solubility and diffusivity compared to the solute. The use of diffusion as the primary transport model allows for the use of Equation 1 to calculate water flux through the membrane. Equation 1 shows that the driving force for solvent flux across the membrane is the difference between the applied pressure difference across the membrane and the osmotic pressure difference across the membrane, and it is proportional to the solvent permeability constant which must be determined experimentally for each membrane [11]. The osmotic pressure is a colligative property of a solution, meaning that it is based on the molar concentration of dissolved solute particles, in this case salt ions, but not the type of solute. It is the driving force of osmosis described by the entropic force pushing solvent molecules to travel from an area of high concentration to an area of low concentration to decrease the concentration gradient. This can be reversed, as the name reverse osmosis suggest, by applying a pressure greater than the osmotic pressure as the driving force. Equation 2 shows that the osmotic pressure of a solution is the product of the concentration of solute ions in solution, the ideal gas constant, and the absolute temperature [11]. Therefore, if the permeability constant for a membrane is known, the solvent flux can be calculated based on the applied pressure difference and concentration difference between the feed and permeate streams.

$$N_w = A_w(\Delta P - \pi_{feed} - \pi_{permeate}) \qquad \text{Equation 1}$$

N_w = solvent flux

A_w = solvent permeability constant

ΔP = pressure difference across the membrane

π = osmotic pressure of solution

$$\pi = cRT$$ Equation 2

π = osmotic pressure of solution

c = molar concentration of solution

R = ideal gas constant

T = absolute temperature

One of the major problems that decrease the efficiency of RO systems is concentration polarization (CP). CP is an increase in solute concentration in the solution near the membrane surface. This can be seen in Figure 7, which shows the solute concentration in various regions near an RO membrane with water flowing from right to left [10]. As seen on the right side of the diagram, solute concentration is assumed to be constant in the bulk region, and then increases near the membrane surface as CP. From there, solute concentration in the dense skin layer as seen in the diagram is drastically lower than in the concentration polarization region due to the low solubility of the solute into the membrane. The concentration gradient in the skin layer is due to the lower diffusivity of the solute compared to that of the solvent. In the porous support layer it can be seen that the solute concentration is essentially the same throughout, which is because the pores are relatively large compared to the size of both water and salt molecules and both have relatively high diffusivities compared to the skin layer.

CP is added into Equation 1 as shown in Equation 3 [11]. Use of this equation shows that as CP increases, the water flux in the permeate or freshwater stream decreases

because the CP acts to decrease the difference between the applied pressure and osmotic pressure by increasing the osmotic pressure on the feed side. Therefore, to achieve the same flux as under conditions of no CP, a higher applied pressure would be required and therefore a higher energy input. The effects of CP can be seen in Figure 8, which shows the normalized polarization ratio as a function of the length of the RO module and system pressure [12]. It can be seen that as pressure increases there is a higher CP ratio. This is due to the fact that the solution is being forced against the membrane more strongly and therefore water is dissolving more rapidly into the membrane, leaving higher concentrations of salt to increase the amount of CP.

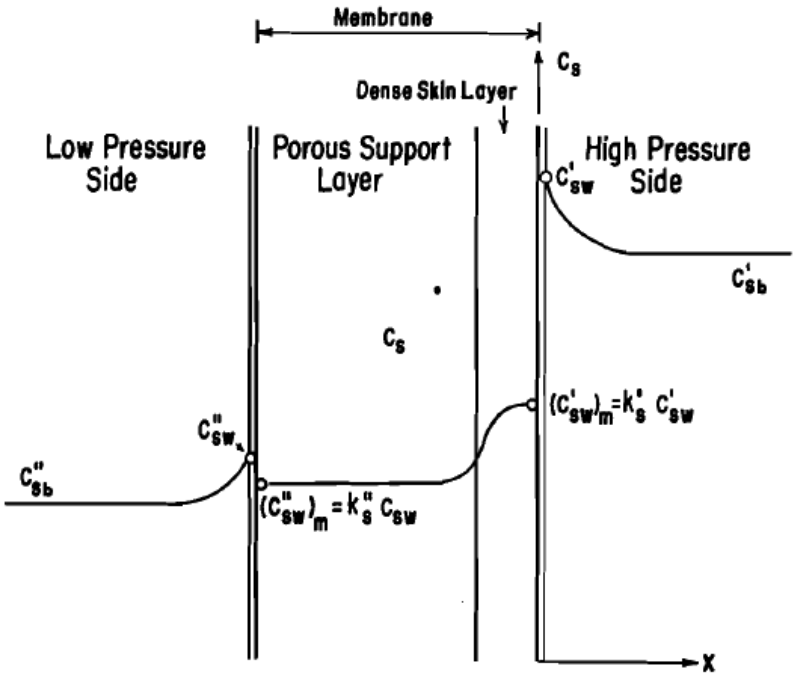

Figure 7: A schematic of solute transport through an asymmetric RO membrane. The figure also shows formation of a CP region at the membrane-solution interface through the local buildup of ions causing an increase in the ion concentration at the membrane surface [10].

$$N_w = A_w(\Delta P - \beta\pi_{feed} - \pi_{permeate}) \qquad \text{Equation 3}$$

B = concentration polarization, defined as the ratio of salt concentration at the membrane surface to the salt concentration in the bulk feed stream, c'_{sw}/c'_{sb} in Figure 7.

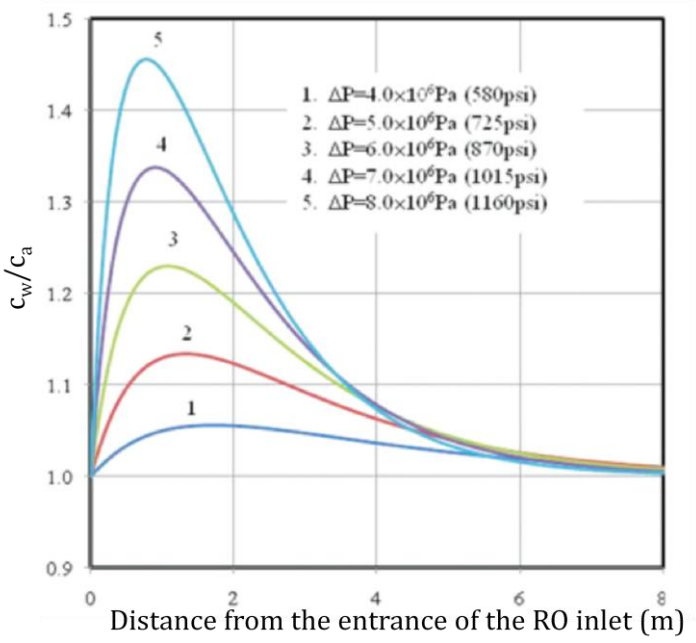

Figure 8: Polarization factor along a typical seawater desalination RO channel under various applied pressures [12].

There are various methods of decreasing the amount of CP near the RO membrane surface, most of which involve increasing the turbulence of the flow near the membrane [12]. The main aim is to increase mixing between the polarization region and the bulk fluid. One of these methods is to increase the fluid velocity, which in turn increases turbulence near the membrane surface and acts to stir the solution, decreasing its salt concentration to near that of the bulk solution. Another method is to decrease the solute concentration, which would in turn decrease the concentration of the CP region. However,

this method also requires the addition of water to dilute the seawater solution, either through a recycle of freshwater from the process or addition of external freshwater, which would increase the pumping requirement and therefore the energy requirement. A third method is to use transverse flow instead of direct flow, so the feed water flows parallel to the membrane surface rather than perpendicular to it. This method is also to increase turbulence near the membrane surface and is currently utilized by spiral-membrane RO systems, as seen in Figure 9 [13].

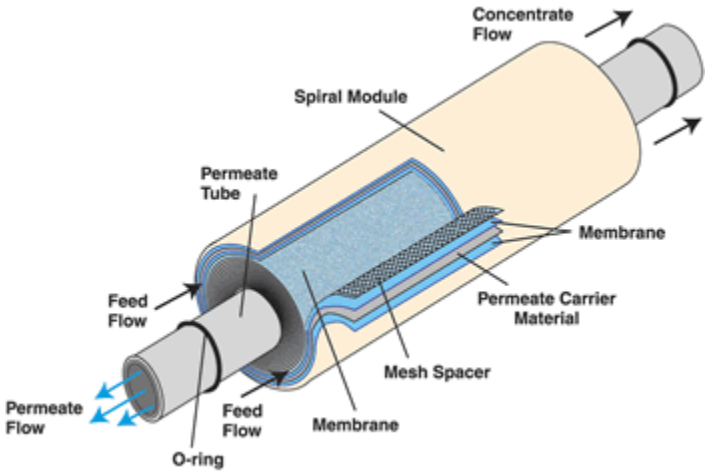

Figure 9: A diagram of a spiral membrane RO module [13].

Another method that is used to mitigate concentration polarization is the use of an ultrasonic frequency to increase turbulence in the solution. It has been shown that the use of a 28 kHz frequency can increase the water flux through a membrane by approximately 50% under continuous application. It has also been shown that a cleaning cycle using a 28 kHz frequency can increase the post-cleaning water flux 200% more than a cleaning cycle with no ultrasonic cleaning stage [14].

It has been shown by Rubinstein and Zaltzman that electro-osmotic convection can be induced at the surface of a permselective membrane, thereby increasing the level of turbulence in the flow near the membrane surface [15]. However, polymer membranes are inherently insulating and therefore do not conduct electrical current. A method to metalize polymer membranes has been developed by Martin, and can allow for the conduction of an electrical current across the surface of an otherwise nonconductive polymer membrane surface [16].

The rest of this thesis details the design and fabrication of the RO test module. The testing and troubleshooting methods are also described. Results from functionality testing of the module are provided and discussed, as well as results from tests incorporating an applied electrical bias. Finally, a brief description of future work for this project is included.

2. MATERIALS AND METHODS

2.1 OVERVIEW

All design work for this project was done in SolidWorks (Dassault Systemes S.A., France). The initial prototype was based on schematics for a disc-tube (DT) reverse osmosis (RO) unit provided by Pall Corporation (Type 02191, USA). The project here is part of a larger project in the Prakash lab where a more energy efficient and smaller desalination system (operates at 375 W for 75 gal/h water output and weighs no more than 20 kg) is being developed for the U.S. Department of Defense. Given these considerations and the ability to easily modify the DT module design, we chose the Pall module as a model system for our study. After the design was completed in SolidWorks, the system was constructed via rapid prototyping using a three-dimensional fused deposition modeling printer available in the Department of Mechanical and Aerospace Engineering at The Ohio State University. Fused deposition modeling operates by extruding thin strands of molten polymer (ABS plastic) in layers to build up the design in an additive fashion. The polymer is then heated, which fuses the strands together to form a solid part.

All solid chemicals were massed using an OHAUS Explorer Pro analytical balance. An Accumet AP85 meter was used for conductivity and pH measurements. All deionized (DI) water was obtained using a Millipore Direct-Q UV system and was purified to a resistance of 18.2 MΩ/cm at 25°C.

2.2 DESIGN BASIS

The Pall DT RO module used as a basis for the design of this project is depicted in Figure 10 [17]. The disc-tube layout consists of a stack of circular layers on top of one

another centered on a tie rod and held together by a nut at each end. The bottom nut pushes on the tie rod spacer, which in turn presses up against the end flange. The end flange is sealed against seal bush with an o-ring (McMaster-Carr, USA), and the seal bush is then sealed against the first hydraulic disc (spacer disc) with another o-ring. On top of the first hydraulic disc is an o-ring, the membrane stack, another o-ring, and then another hydraulic disc, and this sequence is repeated for the desired stack length. When the module is long enough for design constraints, the connection flange is sealed against the top hydraulic disc with an o-ring. The connection flange contains the feed inlet and concentrate outlet ports. The permeate collector is sealed against the connection flange with an o-ring and a nut is used to keep the system at the design length under pressure. A cylindrical pressure vessel is then slid down over the stack, and two lip seals, one in the end flange and one in the connection flange, are used to seal against the pressure vessel. The membrane stack in the Pall system consists of an RO membrane with the skin side down, a fleece sheet, and then another RO membrane with the skin side up. The two membrane sheets are heat pressed, causing them to slightly melt and fuse together.

The water flowpath can be seen in Figure 11, and is such that seawater flows through the feed inlet port, down around the outside of the stack of internal components, and then back up in a zig-zag fashion, flowing parallel to each membrane stack and hydraulic disc face. This way the water crosses over the face of each individual RO membrane. The concentrated brine reject stream then flows out through the concentrate outlet. As the brine stream flows over the RO membranes, some of the water passes through the membrane face and into the volume between the two membranes that is maintained by the polymer mesh. The polymer mesh acts as a spacer between the two

membrane sheets but is porous and allows the purified water to flow laterally into the center of the module, where it then flows vertically up to the permeate outlet. The flow of water through the membrane and into the channel created by the polymer mesh is shown in Figure 12.

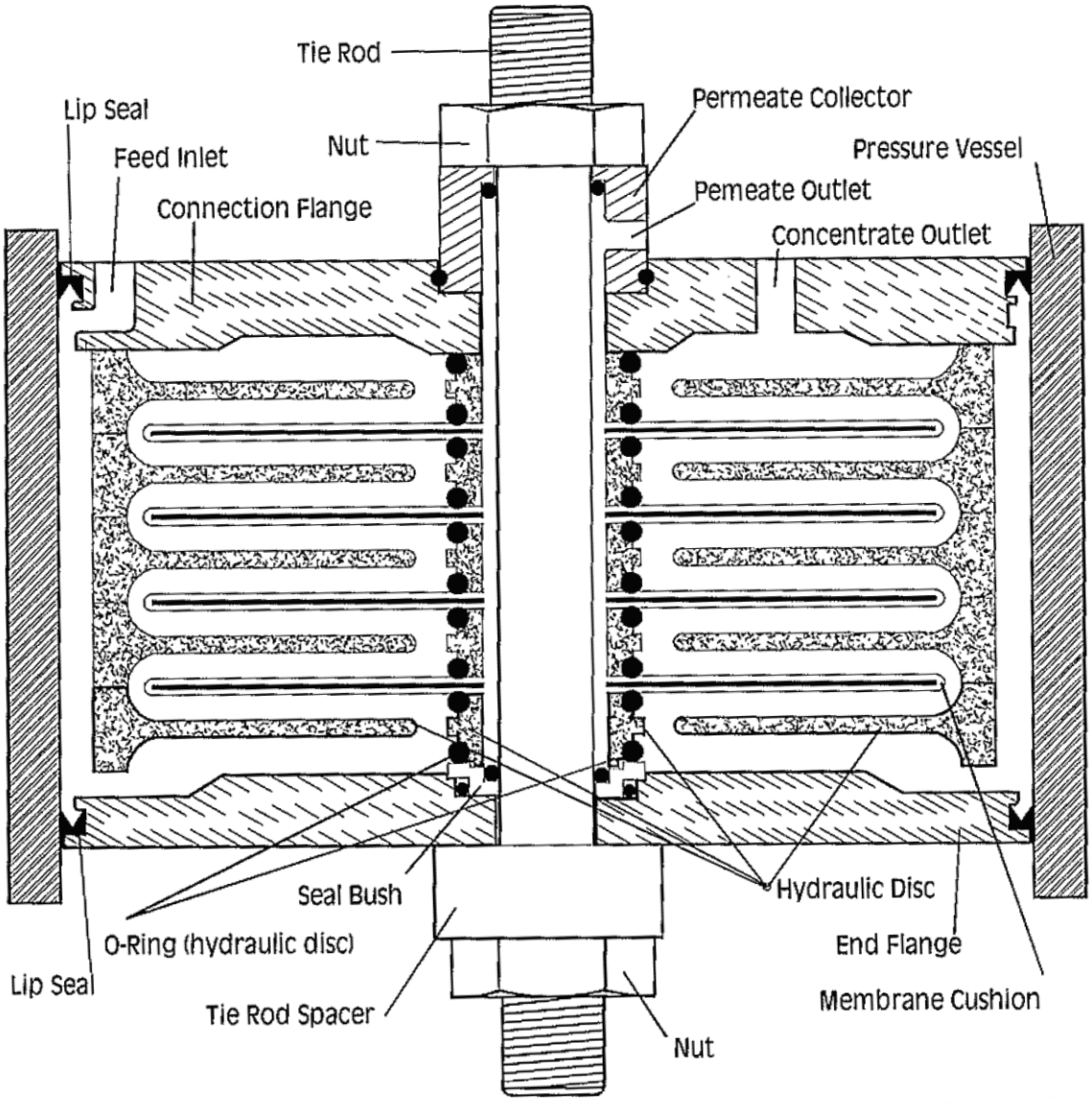

Figure 10: A cross-sectional view of the Pall RO module [17].

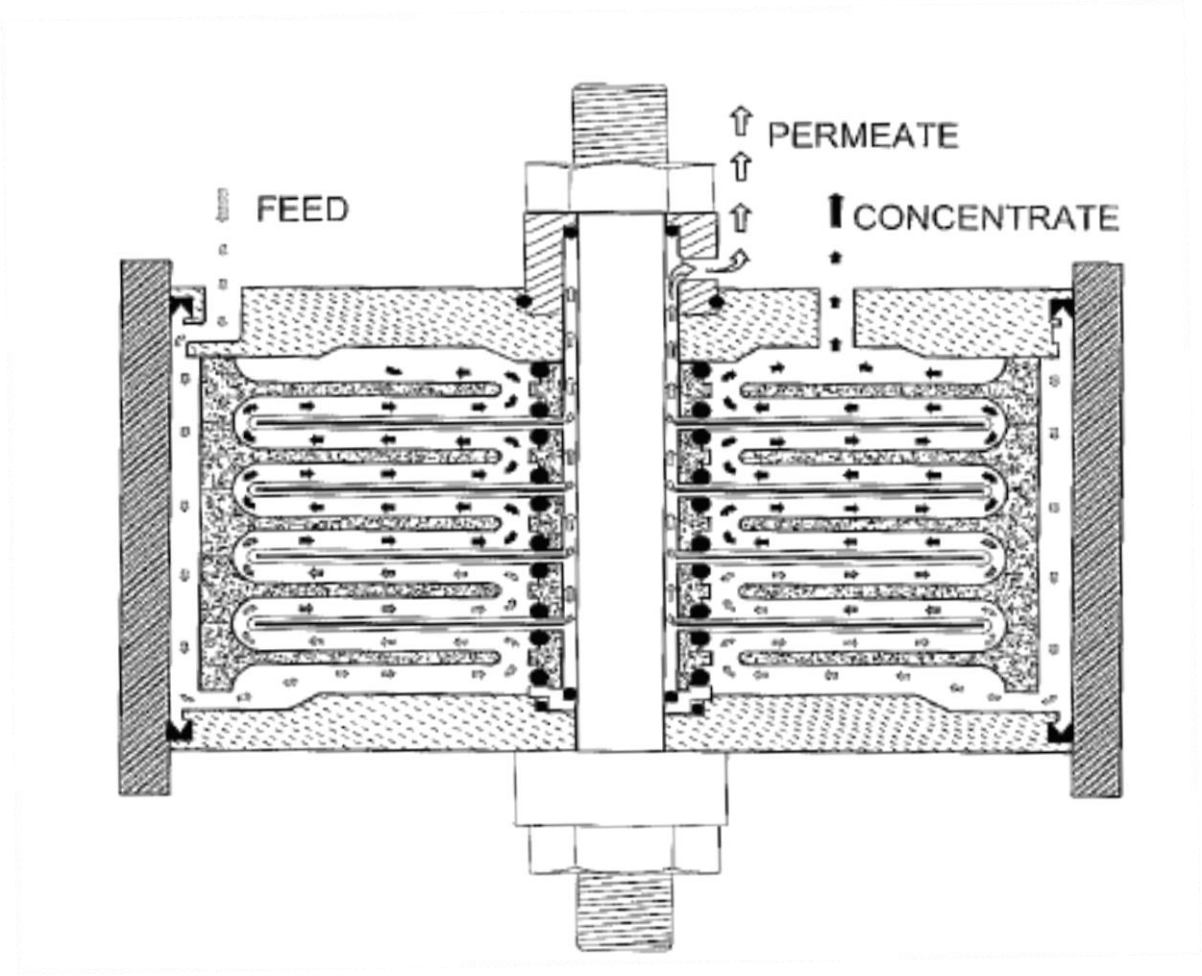

Figure 11: A diagram of water flow through the RO module [17].

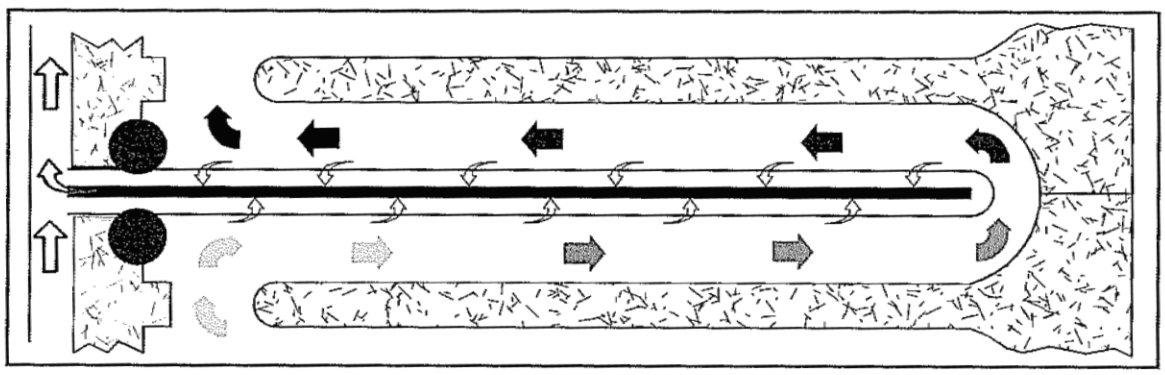

Figure 12: A diagram of water flow through the RO membrane [17].

2.3 SYSTEM LAYOUT

The RO module test system consists of a feed tank, from which water is pumped through the RO module. There are two pressure gauges (Perma-Cal, USA), one located on the feed line between the pump and the module and the other on the reject line. Plastic 3/8" OD tubing (McMaster-Carr, USA) was used for all lines. A bypass line is located before the RO module and is controlled with a ball valve that can be closed to supply feed solution to the module. There is another ball valve on the reject line that can also be closed partially to build up pressure in the module. The two pressure gauges allow for monitoring of the internal system pressure. The first pump used was a self-priming utility pump rated for up to 50 psi (Pacific Hydrostar, USA). The current pump in use is an Aquathin Corp. centrifugal pump (model CDP 8800/XF-PBA, USA). A schematic of the system layout is shown in Figure 13 and a photograph of the system is shown in Figure 14.

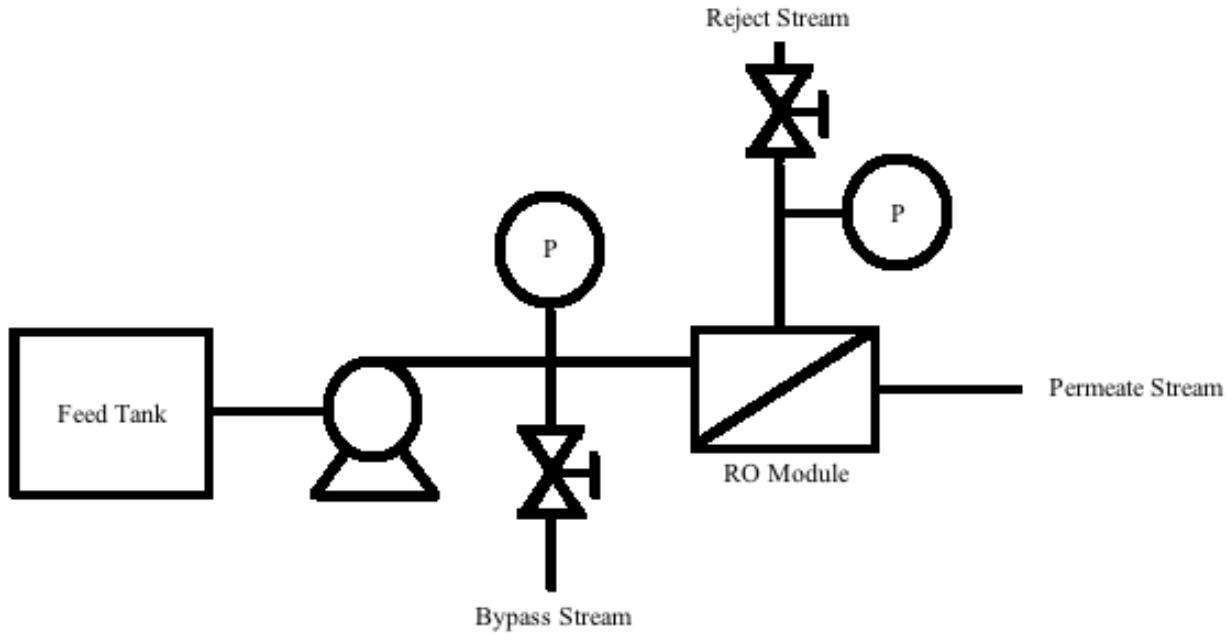

Figure 13: A schematic of the RO module test system.

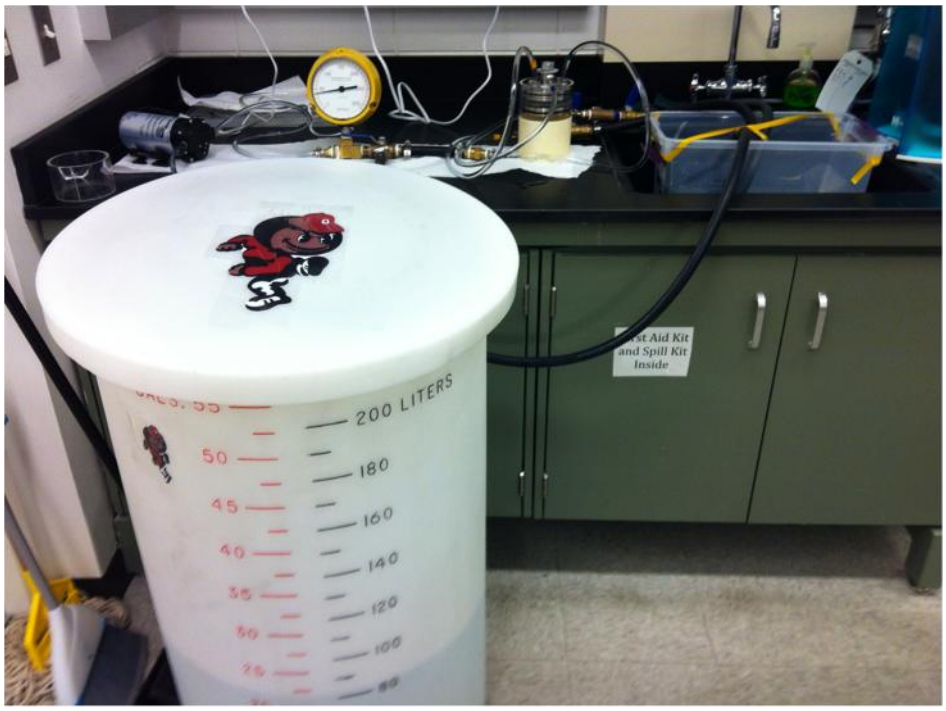

Figure 14: A photograph of the RO module test system. The feed tank is shown in the foreground, and the pump, feed side pressure gauge, and RO module can be seen in the background.

2.4 MEMBRANE STACK MANUFACTURING

The membrane stacks used in the module consist of an octagonal piece of RO membrane skin-side down, followed by a plastic mesh spacer, a piece of steel mesh which was used as the anode in tests in which an electrical bias was applied, another plastic mesh spacer, and finally a second RO membrane, this one skin-side up. All of the internal components were cut approximately 5 mm smaller radially than the RO membranes so when the membranes were heat pressed there was room for them to seal without having the sealing region overlap any of the internal components. A digital photograph of a sealed membrane stack can be seen in Figure 15. FILMTEC™ flat sheet SW30HR RO membranes were used to manufacture the membrane stacks (Dow Water and Process Solutions, USA).

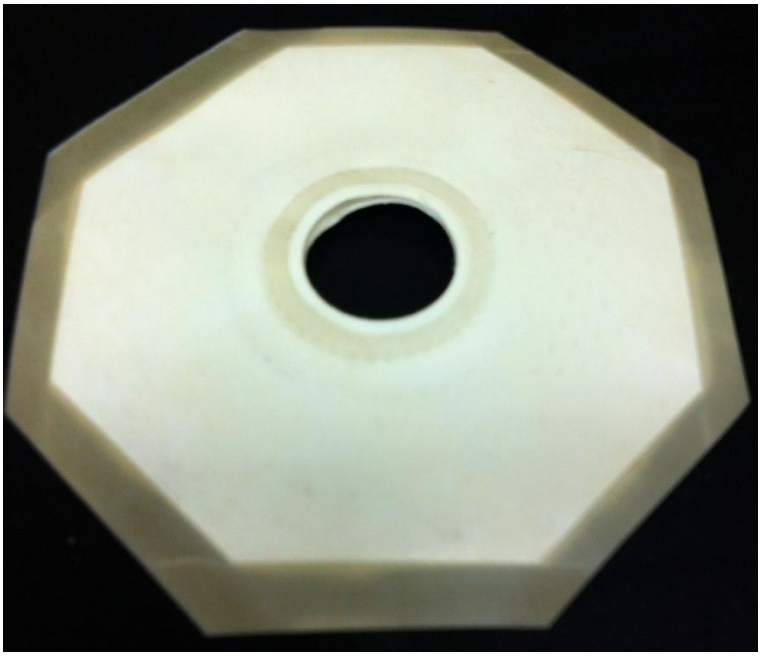

Figure 15: A digital photograph of a membrane stack. The stack measures approximately 85 mm in diameter at its widest distance.

2.5 GOLD PLATING PROCEDURE

The RO membranes were gold plated to enable them to conduct an electrical current. This was done by using a procedure developed by the Martin group, a full step-by-step procedure for which can be seen in Appendix A [15]. Membrane stacks assembled as shown above were placed in metal holders and cleaned in methanol for 5 minutes. The membrane was then soaked in a tin solution consisting 150 mL methanol (Fisher Scientific, USA), 150 mL DI water, 1.50 g $SnCl_2$ (Fisher Scientific, USA), and 1.50 mL trifluoroacetic acid (Acros, USA) for 45 minutes and then cleaned again in methanol for 5 minutes. The membrane was then soaked in a silver solution consisting of 300 mL DI water, 1.8 g $AgCl_2$ (Fisher Scientific, USA), and approximately 50 drops of NH_4OH (Fisher Scientific, USA) for 5 minutes and then cleaned again in methanol for 5 minutes. Then the membrane was soaked in the gold solution composed of 300 mL DI water, 0.630 g $NaHCO_3$ (Fisher

Scientific, USA), 4.8 g Na_2SO_3 (Fisher Scientific, USA), 16.5 mL HCHO (Acros, USA), 7.50 mL electroless gold solution (Technic Inc., USA), and enough drops of H_2SO_4 (Fisher Scientific, USA) to obtain a solution of approximately pH 10 (about 45 drops) for 2 hours in the refrigerator. Finally, the membrane was removed from the metal holder, soaked in DI water for 3 minutes, soaked in HNO_3 (Mallinckrodt Chemicals, USA) for 14 hours, and rinsed in DI water again for 3 minutes. A gold plated RO membrane can be seen in Figure 16.

Figure 16: A gold plated RO membrane.

2.6 DESALINATION TESTING

Salt solutions were made for desalination testing using various concentrations of NaCl (Fisher Scientific, USA) in DI water or Instant Ocean® (Instant Ocean, USA) sea salt formulation. Concentrations were mixed in generally ppm concentrations and 1 gram of salt per liter was equivalent to 1000 ppm. Most tests were run 2000 ppm.

3. RESULTS AND DISCUSSION

3.1 PROTOTYPES

3.1.1 PROTOTYPE I

Prototype I was developed based on a simple scaling-down of SolidWorks files received from Pall Corporation. Only one membrane section supported by two hydraulic discs was used for simplicity, as the main aim is a proof-of-concept demonstration for the polarization mitigation. The scaling resulted in a system diameter of 103 mm. However, this also resulted in a hydraulic disc depth of 2.30 mm, with an o-ring seat depth of 0.20 mm, much less than the 2.50 mm diameter of the o-ring. This depth change led to a poor seat for o-rings used to seal between the membrane and the spacer disks, and therefore a poor seal as the o-rings would become dislodged from their seats and not line up correctly. Also, the thickness of the o-rings caused the thickness of the stack created by the membrane, hydraulic discs, connection flange, and end flange to be too thick for the pressure vessel, as shown in Figure 17. Due to the poor internal sealing of the o-rings, concentrated salt water exited through both the concentrate outlet and permeate outlet.

The applied driving force was a pressure gradient created by gravitational potential force of water in an elevated bucket. This yielded an applied pressure of approximately 20 psi. However, the osmotic pressure difference between a 2000 ppm NaCl solution and a pure water solution is approximately 12 psi. Therefore, the driving pressure, equal to 8 psi or the difference between the applied pressure and the osmotic pressure difference, was not high enough to create a substantial permeate flow rate as a typical RO membrane is rated to run at 800 psi (over-pressure of 400 psi over nearly 400 psi seawater osmotic pressure).

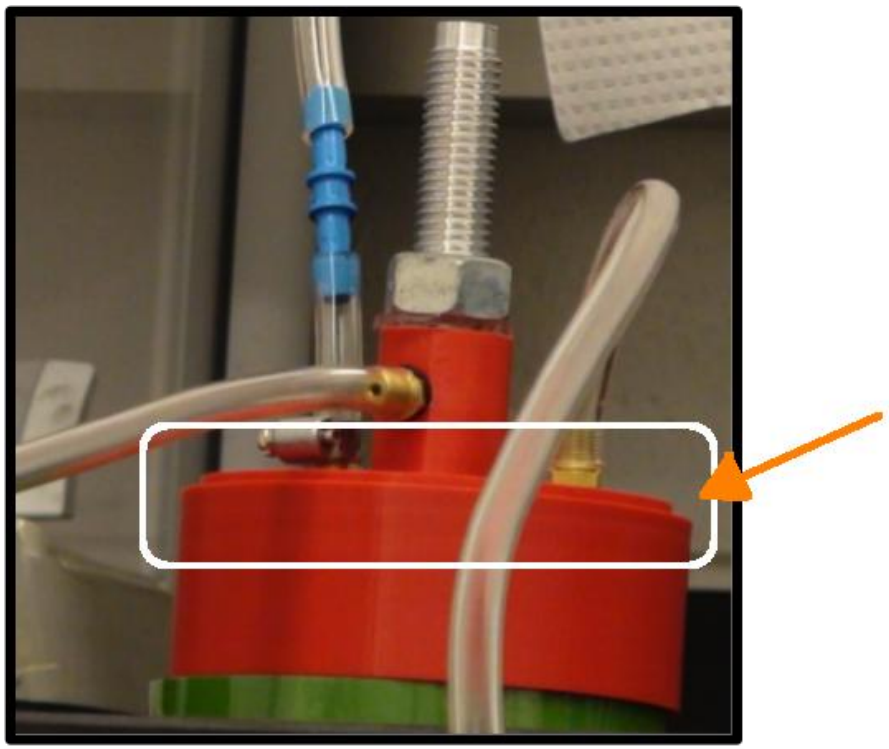

Figure 17: The top of the connection flange can be seen sticking out of the pressure vessel due to the thickness of the o-rings internally, as indicated by the arrow.

3.1.2 PROTOTYPE II

For the second prototype a longer pressure vessel was also fabricated to allow for the extended length of the spacer disks and the width of the o-rings. Hydraulic discs with the same diameter of those used for prototype I (93.06 mm) but with a thickness of 5.0 mm were fabricated to assist with internal o-ring alignment. The fins that form the o-ring seat were adjusted to a depth of 1.80 mm and a width of 1.70 mm to allow the o-rings to fit snugly in the o-ring seat, holding them in place. The utility pump was also incorporated to allow for a greater applied pressure. Due to the increased pressure applied by the pump and the rapid prototyping fabrication of the module parts, water began to leak through the connection and end flanges of the module, parts that are supposed to be solid and watertight. This was due to inadequacies of the fused deposition modeling method. The

strands laid down by the 3D printer were not fused together to form a solid, watertight part, either due to the strands being too thick or the temperature not being high enough to melt the strands completely together. This leaking can be seen in Figure 18. At this higher pressure there was also apparent leaking between the cylindrical casing and the top plate.

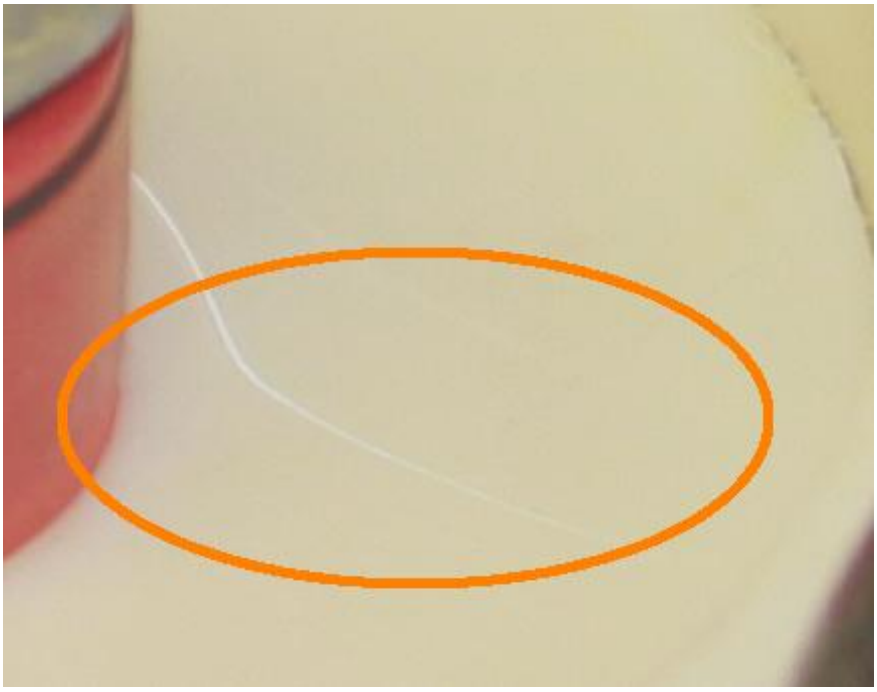

Figure 18: Leaking through the connection flange of the RO module due to rapid prototyping fabrication.

3.1.3 PROTOTYPE III

Development of the third prototype included the design of a connection flange with a lip to contain an extra o-ring seat to prevent leaking between the pressure vessel and the connection flange. The connection flange with the lip and extra o-ring seat can be seen in Figure 19. However, under applied pressure, vibrations in the system caused by the oscillations of the pump caused the pressure vessel and connection flange to vibrate against each other. This vibration created a vertical force on the connection flange, causing

it to lift off of the pressure vessel and increasing the amount of leaking between those two parts. Acrylic boat sealant was used a potential solution to the leaking through the connection and end flanges. However, this solution was unsuccessful and leaking through these two pieces continued to occur, although at a slower rate. Conductivity measurements showed that this prototype was unsuccessful due to the misalignments caused by the vibrations from the pump.

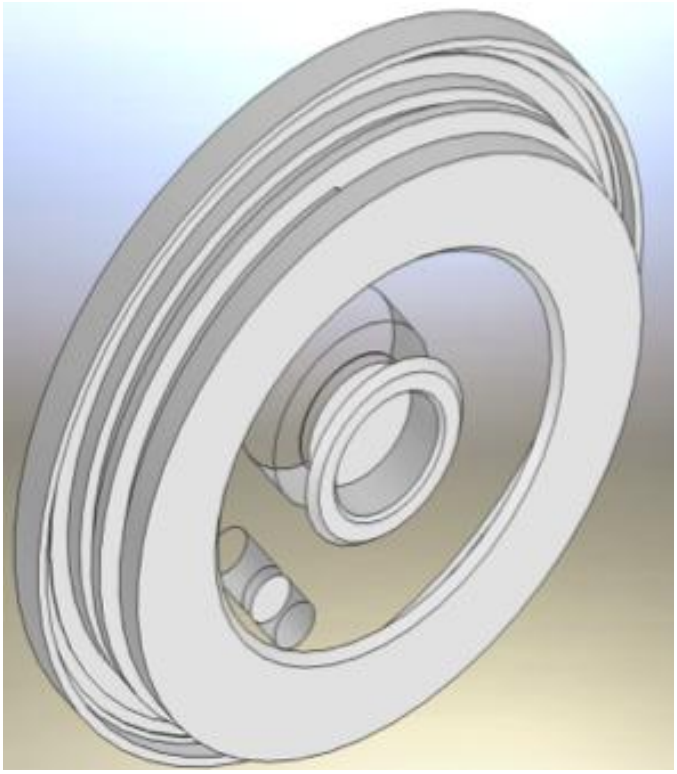

Figure 19: Prototype III connection flange with lip and extra o-ring seat.

3.1.4 PROTOTYPE IV

For the fourth prototype, a clear acrylic pressure vessel was implemented to allow for visual verification of the water flowpath through the module and proper alignment of internal components such as the hydraulic discs and o-rings. Gaskets made of

polydimethylsiloxane (PDMS, Dow Corning, USA) were fabricated in an attempt to reinforce sealing with the central o-rings. Locator pins were also inserted into the hydraulic discs to ensure proper alignment of the internal components. In order to prevent the vibration force on the connection flange that was seen with the third prototype, clamps were used to force the connection flange down onto the pressure vessel, as seen in Figure 20. Leaking though the rapid prototyped connection and end flanges was still a problem for this prototype. Acrylic boat sealant use was continued in an attempt to prevent this leaking. A clamp was also used in an attempt to control the system pressure by preventing flow through the concentrate outlet tubing.

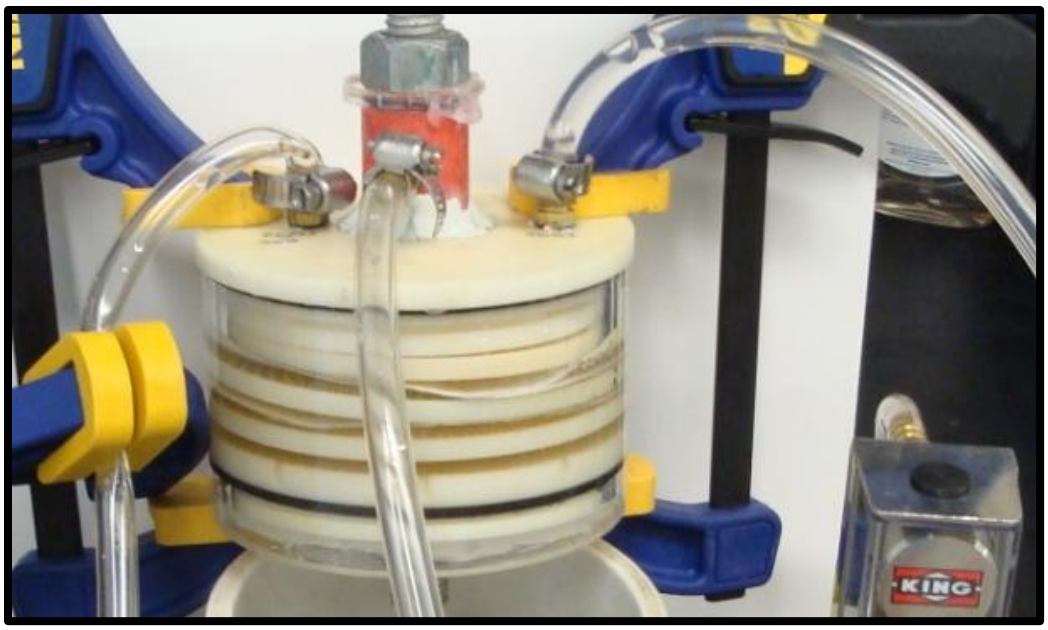

Figure 20: A photograph of prototype IV, showing the clamps used to hold the connection flange onto the pressure vessel.

3.1.5 PROTOTYPE V

The connection flange, the end flange, and the permeate collector were manufactured from stainless steel for prototype V. This finally prevented leaking through the connection and end flanges under operating pressure. A new centrifugal pump rated up to 150 psi was also incorporated to allow for higher operating pressures. The lip was also removed from the connection flange to prevent the vibration problems seen in prototypes III and IV, and presumably due to the use of a stiffer material in the stainless steel, the leaks between the connection flange and pressure vessel seen in prototype II were not seen in prototype V. Quick tube connects were also incorporated in the connection flange and in the plumbing connections leading from the pump to the feed inlet to allow for easier and quicker system setup. The seal bush was also combined with the end flange to reduce a potential source of leaking. A port was added to the connection flange to support the addition of electrical wires for connections to the metalized membrane surface.

During early testing of prototype V showed lower than expected salt rejection, as shown in Table 2. The system was disassembled and examined, and it was found that there were cracks in the hydraulic discs, as shown in Figure 21. It was established that these cracks were allowing bulk feed water to pass through into the permeate stream, causing the higher concentration of salt in the permeate stream.

Table 2: Early prototype V desalination test results.

	Test 1	**Test 2**	**Test 3**
Bulk	3.56 mS	3.56 mS	3.56 mS
Permeate	1.56 mS	1.58 mS	1.48 mS
Reject	3.57 mS	3.57 mS	3.58 mS
Flux rate (L/m^2 *h)	3.59 L/m^{2}h	3.58 L/m^{2}h	3.61 L/m^{2}h

New hydraulic discs were ordered and the thickness of each individual piece in the stack was used to calculate the uncompressed thickness of the module. Then the thickness of the module with an o-ring compression of 40% was calculated and the module was reassembled and compressed to the calculated thickness by tightening the top nut. A torque wrench was used to determine the torque at ideal compression, which was found to be approximately 85 inch-pounds. Therefore, this torque could be used to tighten the module to a consistent compression from assembly to assembly.

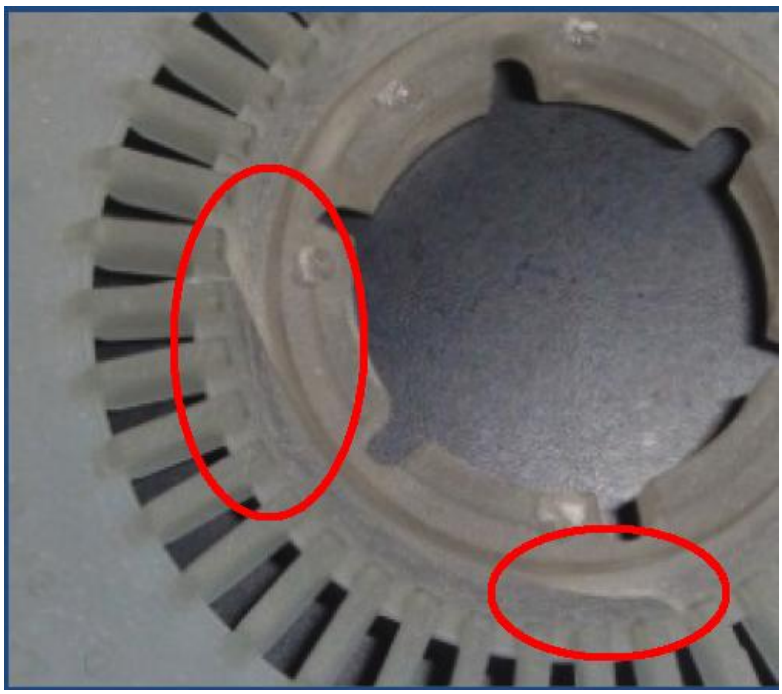

Figure 21: Cracks in the hyrdaulic disc can be seen as indicated by the ovals.

The hydraulic discs were replaced and the desalination tests were rerun, but rejection results were even worse than the previous trials. In order to determine if there was a problem with the internal flowpath of the module, methylene blue was added to the feed solution to act as a dye. Methylene blue is a large organic molecule that is much larger than the pore size of the RO membranes, and therefore should not transport across the membrane. However, when the system was disassembled and the inside of the membrane stack was examined, it was found to have patches of methylene blue covering the inside surfaces of the membrane stack, as seen in Figure 22. Thick bands of methylene blue were also observed around the edges of the membrane on the outside of the stack as well, indicating that there could have potentially been areas of leaking through the membrane. The membranes were replaced and the methylene blue test was rerun, and the results

indicate that the first set of membranes were faulty due to the absence of methylene blue from the inside of the membrane stack, as seen in Figure 23.

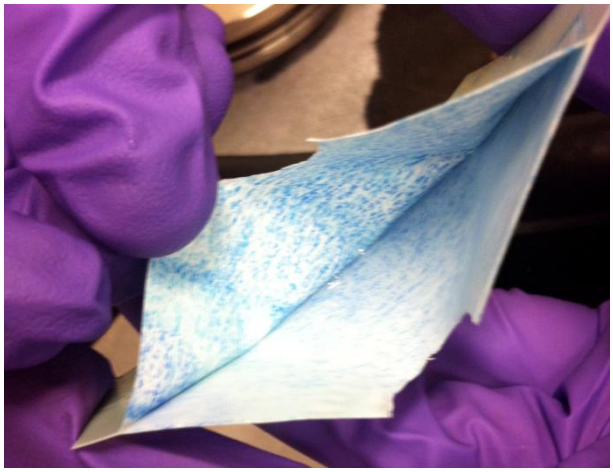

Figure 22: Results of the first methylene blue test. Methylene blue can be seen all over the inside of the membrane stack suggesting failure of the membrane to reject the dye and cause a successful filtration operation.

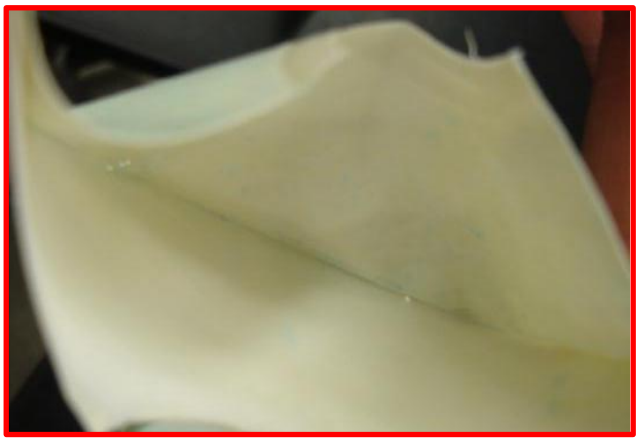

Figure 23: Results of the second methylene blue test. The absence of methylene blue staining indicates that the membranes used in the first test were faulty.

3.1.6 DESALINATION TESTING

The module was reassembled with new membranes and the desalination tests were rerun. The results of these tests show much higher rejections of up to 90%, which is proof

of the functionality of the RO module. Therefore, preliminary applied bias testing was begun. Substantial electrical connections to the gold plated membrane surface could not be maintained due to peeling of the gold layer under minimal force. Therefore, thin pieces of steel mesh were placed above and below the membrane stack. These steel mesh pieces acted as the cathodes to the anode steel mesh piece contained within the membrane stack as previously mentioned. The initial results from these tests show an enhancement of permeate flux that is directly related to increased power consumption as shown in Figure 24. This means that to achieve a higher flux, more power must be consumed and therefore a higher cost for energy must be paid. However, the amount of power consumed to increase permeate flux through CP mitigation may be less than the power required to increase the system pressure to overcome CP resistance. However, more testing needs to be done to confirm these results and confirm these theories.

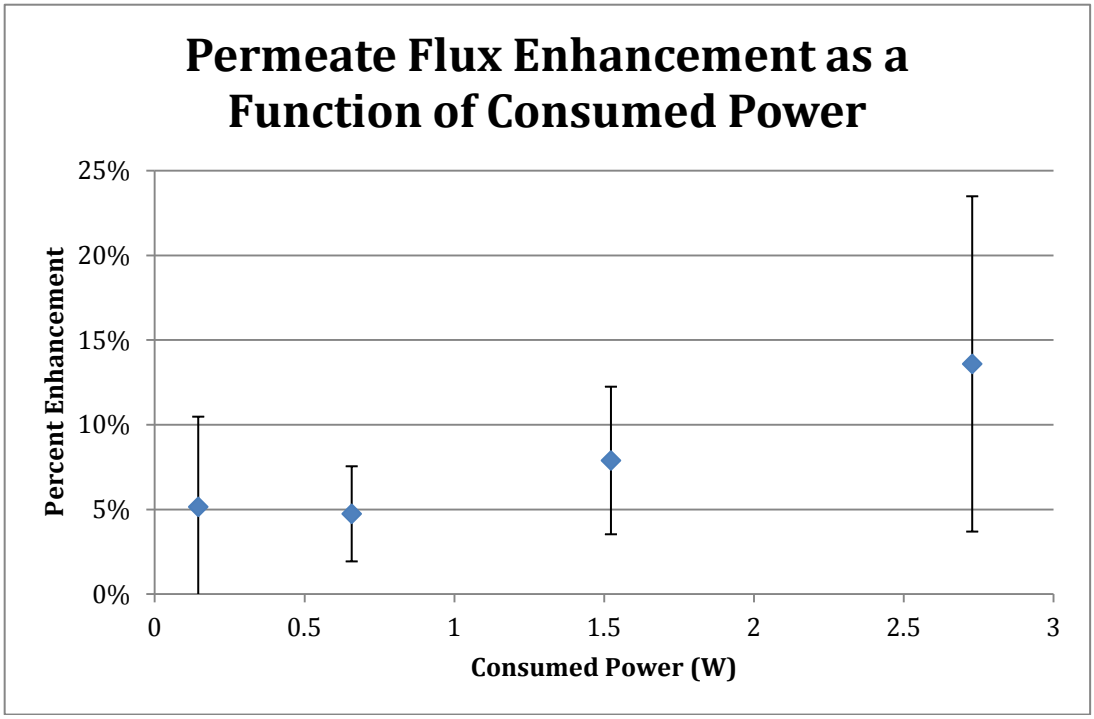

Figure 24: Results of applied bias testing showing improved permeate flux as a function of consumed power.

4. CONCLUSIONS AND FUTURE WORK

A laboratory bench scale modified-DT RO module was developed for use in laboratory testing. The functionalities of several prototypes were assessed until a working model capable of producing salt rejections near 90% was achieved, which are lower than the typical 99% for standard RO. Ease of assembly and inclusion of the electrical connections were considered during the design stages to achieve a module that is as practical as possible. Problems with leaking led to the stainless steel construction of prototype V and the use of pressure rated quick connects. The final prototype is capable of permeate flux rates of over 21 L/m^2h at rejections near 90%. Results from applied bias testing shows that applying an electrical bias to a steel mesh piece near the membrane surface will increase permeate flux by presumably increasing electro-osmotic convection near the membrane surface and therefore decreasing CP. For the RO system, a flux enhancement of 14% was observed for the 85 mm membrane consuming a total of 2.7 W of power.

Future work for this project will include developing a method of reliably connecting electrical wires to the metalized membrane surface to conduct the electrical current. The metalized membranes will then be able to be used for applied bias testing to determine the effect of applying an electrical bias on the permeate flux. If preliminary results from this project hold, this could be a viable, low-power method for increasing permeate flux in RO systems. This would allow for more efficient, and therefore lower cost, water desalination in regions where freshwater is in need for its myriad uses.

REFERENCES

[1] Oki, T.; Kanae, S. Global Hydrological Cycles and World Water Resources. *Science* **313**, 1068-1072 (2006).

[2] David Molden, ed. Comprehensive Assessment of Water Management in Agriculture. 2007. International Water Management Institute. 3 March 2010.

[3] Prakash, S.; Bellman, K.; Shannon, M.A. Recent Advances in Water Desalination Through Biotechnology and Nanotechnology. In *Bionanotechnology II: Global Prospects.* Reisner, D.E., Ed.; CRC Press, 2011; pp. 365-382.

[4] Confalonieri, U., et al. Human health. Climate Change 2007: Impacts, Adaptation and Vulnerability. IPCC. 2007. Cambridge University Press, Cambridge, UK, 391-43

[5] Service, R. F. Desalination Freshens Up. *Science* **313**, 1088-1090 (2006).

[6] Mayer, P.W., et. al. Residential End Uses of Water, American Water Works Association, 1999.

[7] U.S. Environmental Protection Agency

[8] Veolia Water Solutions & Technologies

[9] American Membrane Technology Association

[10] Mohammad Soltanieh, William N. Gill, Review of Reverse Osmosis Membranes and Transport Models, Chemical Engineering Communications, 1981, 12:4-6, 279-363.

[11] Geankoplis, C.J. Transport Processes and Separation Process Principles, 4th ed. Prentice Hall: Westford, MA. 2010. Pages 883-893.

[12] Song, Lianfa. "Concentration polarization in a narrow reverse osmosis membrane channel." *AIChE Journal* 56.1 (2010), 143 - 149.

[13] GE Osmonics

[14] Ming Cai, Shuna Zhao, Hanhua Liang, Mechanisms for the enhancement of ultrafiltration and membrane cleaning by different ultrasonic frequencies, Desalination, Volume 263, Issues 1-3, 30 November 2010, Pages 133-138.

[15] I. Rubinstein and B. Zaltzman, Phys. Rev. E **62**, 2238 (2000).

[16] Kshama B. Jirage. *The Fabrication of Gold Nanotubular Membranes and their Applications in Separations.* PhD dissertation, Colorado State University, 1999.

[17] Pall Corporation

APPENDIX A

Process for Electroless Deposition of Gold on Nanoporous Membranes

At least the night before:

1. Rinse amber bottle marked for Au solution with DI water.
2. Add 300 mL DI water to the bottle.
3. Add 0.630 g sodium bicarbonate ($NaHCO_3$) to the solution.
4. Add 4.8 g sodium sulfite (Na_2SO_3) to solution.
5. Agitate gently until completely dissolved. Otherwise, sonicate for 15 minutes until dissolved completely.
6. Place in refrigerator.

Plating next day:

7. Clean stainless holder (SSH) and screws acetone followed by IPA followed by methanol using a polyester wipe & polyester q-tip.
8. Clean O-rings with IPA using a polyester wipe.
9. SC-1 clean all metal parts.
    a. 300:30:3 DI Water: Hydrogen Peroxide: Ammonium Hydroxide
    b. Begin hotplate at 400^{o}C, reduce to 250^{o}C when temperature of solution reaches 73^{o}C.
    c. Leave at 73^{o}C for 10 minutes.
10. Rinse well with water.
11. Place membrane on SSH evenly centered taking care not to wrinkle or move membrane.
12. 'Click' the o-ring into place and ensure that the membrane is not ripped or excessively wrinkled. If so, repeat step 11.

Sn Solution:

13. Begin by soaking membranes and holders in MeOH for five minutes.
14. Rinse soaking glassware with DI water followed by methanol.
15. Rinse amber bottle marked for Sn with DI followed by methanol, ensure that no excess liquid is left in the bottle.
16. Rinse measuring cylinder with DI.
17. Add 150 mL methanol to Sn bottle.
18. Add 1.50 g $SnCl_2$ and agitate solution **gently.**
19. Add 1.50 mL trifluoroacetic acid to solution.
20. Sonicate for 1 minute. Check that everything is dissolved.
21. Add 150 mL DI water to solution.
22. Soak membrane and membrane holder in soaking glassware for 5 min.
23. Rinse Sn glassware with DI, ensuring excess liquid is not left. Evenly distribute Sn solution between two dishes and soak membranes for 45 minutes.
24. Move membranes and holders to soak in MeOH for 5 minutes.

Ag Solution

25. Rinse small vial with DI water.
26. Add 15 mL DI to vial.
27. Rinse bottle marked for Ag solution with DI.
28. Add 285 mL DI to bottle.
29. Add 1.8 g $AgCl_2$ to vial
30. Slowly add NH_4OH drop-wise from scintillation vial. Agitate gently after ever 2-3 drops to mix solution evenly till about 50 drops have been added and solution is clear. [Note: Solution turns brown, then a muddy yellow, and clear again.]
31. Add small vial of AgCl to 285 mL.
32. Gently agitate to allow Ag solution to mix well.
33. Evenly distribute Ag solution between two dishes and soak membranes for 5 minutes.
34. Move membranes and holders to soak in MeOH for 5 minutes.

Au Solution

35. Prepare soaking glassware as before.
36. Retrieve Au soln from refrigerator and add 16.5 mL formaldehyde (HCHO).
37. Add 7.50 mL electroless Au soln.
38. VERY gently agitate to allow mixing.
39. Wait about five minutes to check pH, which should be approximately 12.4.
40. If pH is ~12.4, add 42 drops sulfuric acid. [Goal is to drop pH to 10, but not below. Remember, pH is a log scale]
41. Gently agitate and return to refrigerator; wait at least 3 minutes to allow pH to level off before adding more sulfuric acid.
    a. From notes: 11.41 add 8 drops 10.11
    b. 11.17 add 6 drops 10.26
    c. 10.83 4 drop 10.35
    d. 10.59 add 3 drop 10.00
    e. 10.43 2 drop 9.90
42. After completing pH shift, put solution in refrigerator until needed.
43. Evenly distribute Au solution between two dishes and soak membranes for 2 hours in refrigerator.

Nitric Acid Soak

44. Carefully release membranes from holders and o-rings.
45. Place membranes in DI water and soak membranes for 3 minutes. [Tip: membranes will curl and stick, carefully spread out using tweezers.]
46. In acid soaking glass ware, mix 240 mL DI and 45 mL Nitric Acid (HNO_3).
47. Soak for at least 12 hours but not more than 15 hours (~ overnight)
48. Rinse in DI water bath as in step 45.

49. Take membranes out of water, lay on polyester wipe. Flip membrane over on cloth, membrane should be relatively dry now. Now store membranes in dry, clean environment.

Quick Timeline

At least 5 hours before: Prepare initial Au solution to allow it to get cold.

1. 5 minute methanol soak
2. 45 minute Sn soak
3. 5 minute methanol soak
4. 5 minute Ag soak
5. 5 minute methanol soak
6. 4 hour (variable) Au soak
7. 3 minute DI water soak
8. 12-15 hr nitric acid soak
9. 3 minute DI water soak